Applied Energy 87 (2010) 824–835

Contents lists available at ScienceDirect

Applied Energy

journal homepage: www.elsevier.com/locate/apenergy

Experimental investigation and performance analysis on a solar adsorption cooling system with/without heat storage

X.Q. Zhai *, R.Z. Wang

Institute of Refrigeration and Cryogenics, Shanghai Jiao Tong University, Shanghai 200240, China

ARTICLE INFO

Article history:
Received 8 June 2009
Received in revised form 30 September 2009
Accepted 3 October 2009
Available online 30 October 2009

Keywords:
Solar energy
Adsorption cooling
System with heat storage
System without heat storage

ABSTRACT

A solar adsorption cooling system which can be switched between a system with heat storage and a system without heat storage was designed. In the system with heat storage, a heat storage water tank was employed as the link between the solar collector circulation and the hot water circulation for the adsorption chillers. However, the heat storage water tank was isolated in the system without heat storage, and the hot water was directly circulated between the solar collector arrays and the adsorption chillers. It was found that the inlet and outlet temperatures for the solar collector arrays and the adsorption chillers in the system without heat storage were more fluctuant than those of the system with heat storage. Also found was that the system with heat storage operated stably because of the regulating effect by the heat storage water tank. However, under otherwise similar conditions, the cooling effect of the system without heat storage was similar to that of the system with heat storage. Compared with the system with heat storage, the system without heat storage has the advantages of higher solar collecting efficiency as well as higher electrical COP.

1. Introduction

Summer air-conditioning represents a growing market in building services world-wide in both commercial and residential buildings. The main reasons for the increasing energy demand for summer air-conditioning are increased thermal loads, increased living standards and occupant comfort demands as well as building architectural characteristics and trends, like an increasing ratio of transparent to opaque surfaces in the building envelope to even the popular glass buildings [1]. Solar cooling constitutes an interesting technological alternative to cope with the increasing cooling energy demand with sustainability criteria. It has additional advantages like avoiding the use of halogenated hydrocarbons, reducing the impact on the ozone layer, and justifying an increased installed area of low-temperature solar collectors [2].

Currently, most of the solar cooling systems commonly used are hot water driven lithium bromide absorption chillers. Kumar and Devotta described a mathematical model of a solar regenerator, which could be used in either an open-cycle desiccant-cooling system or an open-cycle absorption cooling system [3]. Muneer and Uppal developed a detailed numerical simulation model for a commercially available solar absorption chiller. The study established the high potential of solar operated, water-cooled absorption coolers especially for arid conditions [4]. Mateus and Oliveira used the TRNSYS software to evaluate the potential of integrated solar absorption cooling and heating systems for building applications [5]. Desideri et al. analyzed the technical and economic feasibility of solar absorption cooling systems, designed for two different application fields: industrial refrigeration and air-conditioning. The purpose of this paper was to determine technical solutions for greater energy efficiency, which were also repeatable for companies or users with similar processing cycles [6].

Ali et al. reported the design and performance of a solar absorption cooling system. The system included an absorption chiller with the cooling capacity of 35 kW, vacuum tube collectors with the aperture area of 108 m^2 and a heat storage water tank with the volume of 6.8 m^3. It was reported that the chiller COP varied from 0.37 to 0.81 [7]. Pongtornkulpanich et al. designed a solar-driven 35 kW $LiBr/H_2O$ single-effect absorption cooling system. It was shown that the 72 m^2 evacuated tube solar collectors delivered a yearly average solar fraction of 81% [8]. Rodríguez Hidalgo et al. carried out an experimental research on a solar absorption cooling system. The system was based on an on-Campus field of 50 m^2 flat-plate solar collectors driving a single-effect commercial $LiBr/H_2O$ absorption chiller through a heat storage water tank. Experimental results showed that the cooling power of the system reached 6–10 kW [9]. Syed et al. reported some novel experimental results derived through field testing of a part load solar energized cooling system for a typical Spanish house in Madrid during the summer period of 2003. The solar hot water was supplied by a 49.9 m^2 array of flat-plate collectors, and used to drive a single-effect $LiBr/H_2O$

* Corresponding author. Tel./fax: +86 21 34206296.
E-mail addresses: xqzhai@sjtu.edu.cn, zxqzhai@163.com (X.Q. Zhai).

0306-2619/$ - see front matter © 2009 Elsevier Ltd. All rights reserved.
doi:10.1016/j.apenergy.2009.10.002

Nomenclature

A	area (m^2)
COP	coefficient of performance
C_p	specific heat of water (J/kg °C)
$D1$	duration of the solar collecting system operation (s)
$D2$	duration of the adsorption chillers operation (s)
$D3$	working time (s)
F_i^c	collector control function
F_i^L	load return control function
I	solar radiant intensity ($W\,m^{-2}$)
m	mass flow rate ($kg\,s^{-1}$)
N	number of nodes
Q	heat (kW)
T	temperature (°C)
U	heat loss coefficient (W/m^2 °C)
V	volume (m^3)

Greek symbols

ρ	density of water ($kg\,m^{-3}$)
η	average solar collecting efficiency
Δm	net flow between nodes ($kg\,s^{-1}$)
Δx	distance between nodes (m)

Subscripts

a	ambient
ave	daily average
c	solar collector
chill	chilled water
hp	heat pipe evacuated tubular solar collector
hw	hot water
i	node
in	inlet
o	outlet
pn	pipe network
se	section
si	side
ta	tank
U	U-type evacuated tubular solar collector
w	water
wh	system with heat storage
wo	system without heat storage

absorption chiller of 35 kW nominal cooling capacity. A minimum hot water inlet temperature to the generator of 65 °C was required to commence cold generation. The measured maximum instantaneous, daily average and period average COP were 0.60 (at maximum capacity), 0.42 and 0.34, respectively [10]. Li et al. reported on the performance of a solar-powered absorption cooling system with a partitioned hot water storage tank. The system employed a flat-plate collector array with a surface area of 38 m^2 to drive a $LiBr/H_2O$ absorption chiller of 4.7 kW cooling capacity. The system could attain a total solar cooling COP of about 0.07 [11].

Another potential solar-powered cooling system is the solar adsorption cooling system. The main difference compared to absorption systems is that two or more adsorbers are necessary in order to provide continuous operation. Adsorption systems allow for somewhat lower driving temperatures but have a somewhat lower COP compared to absorption systems under the same conditions. The use of adsorption cooling technology is preferable for minitype solar-powered cooling systems [12,13].

Alghoul et al. reported the conceptual design and performance of a dual-purpose solar continuous adsorption system for domestic refrigeration and water heating [14]. Khattab developed a mathematical model to simulate and optimize the performance of a solar-powered adsorption refrigeration module with the solid adsorption pair of charcoal and methanol [15]. Saha et al. analyzed a dual-mode silica gel/water adsorption chiller which utilized effectively low-temperature solar or waste heat sources of temperature between 40 and 95 °C. Two operation modes were possible for the advanced chiller. The first operation mode worked as a highly efficient conventional chiller where the driving source temperature was between 60 and 95 °C. The second operation mode worked as an advanced three-stage adsorption chiller where the available driving source temperature was very low (between 40 and 60 °C). The simulation results showed that the optimum COP values were obtained at driving source temperatures between 50 and 55 °C in three-stage mode, and between 80 and 85 °C in single-stage, multi-bed mode [16]. Li et al. established a lumped parameter model to investigate the performance of a solar-powered adsorption air-conditioning system driven by flat-type solar collectors. One of the major contributions of the model was its simplicity and convenience in analyzing the performance of such hybrid systems. The proposed model could predict well the dynamic response of adsorption systems for given operational conditions [17].

Up to now, experimental studies on solar-powered adsorption cooling systems were mainly based on the performance of adsorption chillers. Saha et al. experimentally investigated a double-stage, four-bed, nonregenerative adsorption chiller powered by solar/waste heat sources between 50 and 70 °C. The prototype studied produced chilled water at 10 °C and had a cooling power of 3.2 kW with a COP of 0.36, when the heating source and heat sink temperatures were 55 and 30 °C, respectively. Flat-plate solar collectors could easily produce hot water to regenerate the adsorbent of the chiller at this level of temperature [18]. Liu et al. developed an adsorption chiller with the working pair silica gel/water that had no refrigerant valves. This feature reduced the cost of the chiller, and made it more reliable, as there were fewer moving parts, which could allow air infiltration. The sorption bed of such a chiller could be regenerated by hot water of between 75 and 90 °C. The whole chiller contained 52.8 kg of silica gel divided between two adsorbent beds, which operated out of phase and thus, produced continuous cooling. Experiments with the first prototype showed that a cooling power of 3.56 kW and a COP of 0.26 could be obtained when the mass and heat recovery processes were employed under the follow operation conditions: evaporation temperature of 7 °C, heat sink temperature of 28 °C, and heat source temperature of 85 °C. The chiller was especially suitable for solar cooling systems with evacuated tube solar collectors as the source of thermal energy [19]. Zhai et al. reported the solar adsorption cooling system of the green building of Shanghai Research Institute of Building Science. The experimental results showed that the average cooling capacity was 15.31 kW under the typical weather condition of shanghai [20].

The existing solar cooling systems, either solar absorption cooling systems or solar adsorption cooling systems, are always the systems with heat storage. These systems include the heat storage water tanks which accumulate heat by solar collecting circulation. The chillers are then driven by the hot water from the heat storage water tanks. Such systems have been reported by Ali et al. [7], Pongtornkulpanich et al. [8], Li and Sumathy [11], Zhai et al. [20], and the like.

Few reports have been found to be systems without heat storage. Compared with a system with heat storage, a solar cooling sys-

tem without heat storage has the advantage of simplicity because of nonuse of the heat storage water tank. In such systems, the chillers are directly driven by the hot water from the solar collectors.

In this paper, a solar-powered adsorption cooling system which could be switched between the system with heat storage and the system without heat storage was designed and set-up to operate in the green building of Shanghai Research Institute of Building Science. The experimental results under different operating modes (the system with/without heat storage) were compared. Moreover, the variations of the system performance under different operating modes were also compared.

2. Experimental set-up

2.1. Installation of the solar collectors

Designed to be a demonstration project, the green building of Shanghai Research Institute of Building Science contains multiple renewable energy technologies, such as solar thermal technology, solar photovoltaic, natural ventilation, natural lighting, indoor planting, etc. Solar energy used to drive the adsorption chillers was collected by 90 m^2 of U-type evacuated tubular solar collectors with compound parabolic collectors installed on the southwest side of the roof, and by 60 m^2 of heat pipe evacuated tubular solar collectors installed on the southeast side. In order to enhance the efficiency utilization of solar energy, the roof was tilted to an angle of 40° to the ground surface. Fig. 1 shows the appearance of the building integrated with solar collectors. All solar collectors of both sides were divided into three parallel rows. The collector units in each row were connected in a serial arrangement for the purpose of achieving hot water with a relatively high temperature, which is important to improve the performance of the system. Such an arrangement of the solar collectors not only guarantees high system performance but also improves the appearance of the building facade.

2.2. Design of the solar cooling system

The solar cooling system was designed and set-up to operate in a building area of 460 m^2. Except for the solar collectors, the solar cooling system was mainly composed of two adsorption chillers, a cooling tower, a heat storage water tank of 2.5 m^3, fan coils inside the air-conditioned rooms and circulating pumps for the solar collectors (Pump 1), hot water (Pump 2) and cooling water (Pump 3). All the components were connected by tubes and valves to form a whole flow circuit, as shown in Fig. 2. By switching the valves, the solar cooling system could be operated in two different operating modes.

Fig. 1. Integration of the solar collector array and the green building.

1. For the system with heat storage, valves V2, V3, V4, V5 and V8 were turned on; however, valves V1, V6 and V7 were turned off. The water tank was employed to store the solar heat, and provided hot water to the adsorption chillers.
2. For the system without heat storage, valves V2, V3, V4, V5 and V8 were turned off; however, valves V1, V6 and V7 were turned on. The water tank and the hot water pump (Pump 2) were isolated. An expansion tank of 0.1 m^3 was installed above the pipe network for the purpose of setting pressure for the system.

In the system with heat storage, the heat storage water tank was specially designed to be the link between the solar collector circulation and the hot water circulation of the adsorption chillers. The hot water from the solar collector arrays flowed into the top of the water tank, and the water returning from the adsorption chillers flowed to the bottom. In addition, the hot water for adsorption chillers came from the top of the water tank. Three platinum resistance sensors were fixed at the top, middle and bottom of the heat storage water tank, respectively. The structure of the heat storage water tank was shown in Fig. 3.

In order to complete the solar-powered cooling system, we chose the environment friendly silica gel/water as the working pair and designed an adsorption chiller, which was capable of working effectively from 55 °C to 95 °C. The chiller can be regarded as one combined by two single-bed systems. It is composed of three vacuum cavities: two adsorption/desorption working chambers and one heat pipe working chamber. There is only one vacuum valve installed, and it allows the mass recovery process between the two adsorption/desorption working chambers. The adsorber is a compact finned-tube heat exchanger, the condenser is a shell and tube heat exchanger, and the evaporator cooling is output through a methanol chamber, which acts as a gravity heat pipe. The cycle process of the adsorption chiller can be described as follows: the heating/cooling time is 900 s, the mass recovery time is 180 s and the heat recovery time is 60 s. The nominal cooling capacity is 8.5 kW when the hot water temperature is 85 °C. See Wang et al. [21] for a detailed account of the adsorption chiller.

2.3. Data acquisition and control system

The whole system was controlled by a computer and operated automatically. The temperatures were recorded by platinum resistance sensors (Pt. 1000, grade A), which were fixed at some main points of the system, either for monitoring or for control. The flow rate was measured by a remote transmitting flowmeter (±3% accuracy in the range of 0–15 $m^3\,h^{-1}$). The insolation was measured by a pyranometer with ±2% of accuracy. The data were recorded at every 15 s by a data logger, which was connected to the computer.

3. Theoretical analysis

3.1. Solar collectors

The useful energy received by the solar collectors can be calculated according to the instantaneous efficiency of two kinds of solar collectors.

The two solar collector arrays were tested on the efficiency characteristics under identical weather conditions to evaluate their respective performance. The instantaneous experimental solar collecting efficiency data were expressed as the function of $(T_{c,in} - T_a)/$

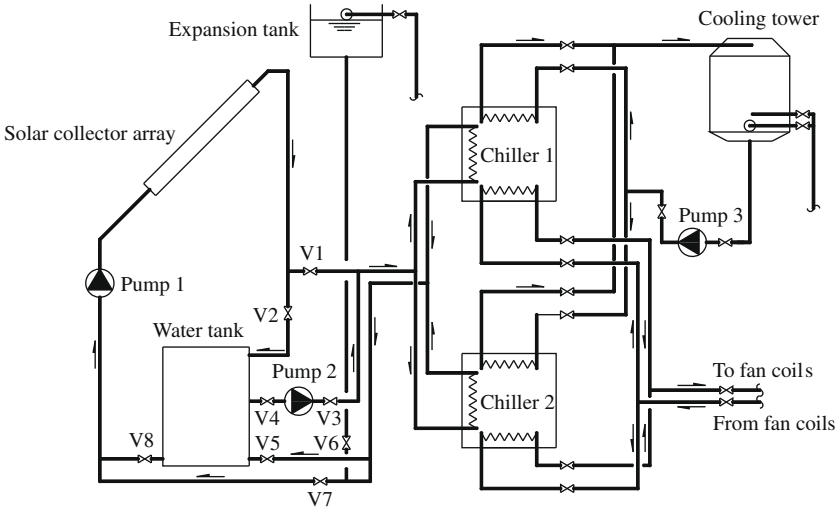

Fig. 2. Flow diagram of solar-powered adsorption cooling system.

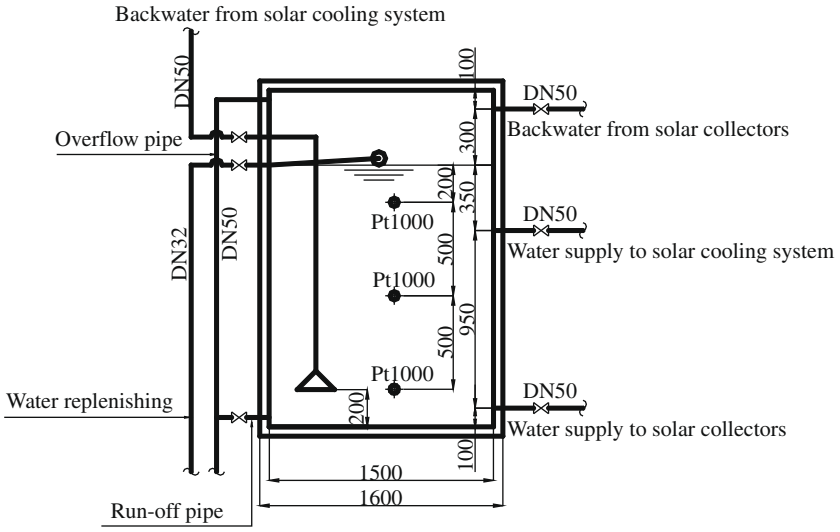

Fig. 3. Structure of the heat storage water tank.

I, as shown in Fig. 4. The instantaneous efficiency for the two solar collector arrays were simulated and denoted as:

For the heat pipe evacuated tubular solar collector array:

$$\eta_{c,hp} = 0.65 - 2.94(T_{c,in} - T_a)/I \tag{1}$$

For the U-type evacuated tubular solar collector array:

$$\eta_{c,U} = 0.45 - 1.10(T_{c,in} - T_a)/I \tag{2}$$

3.2. Adsorption chiller

The heat consumed by the adsorption chiller is expressed as:

$$Q_{hw} = Q_{\text{chill}}/\text{COP} \tag{3}$$

where Q_{chill} and COP can be determined from the temperature of hot water supplied to the adsorption chillers, which is available from the adsorption chiller manufacturer [21].

3.3. Heat storage water tank of the system with heat storage

In the system with heat storage, the heat storage water tank can be considered as a stratified water tank and can be modeled by dividing the tank into N nodes (sections), with energy balances written for each section of the tank. The energy equation takes into account the energy gain from the collectors, energy lost to surroundings and energy consumed by the adsorption chillers. The result is a set of N differential equations that can be solved for the temperatures of the N nodes as a function of time. The simulation model of the heat storage water tank is shown in Fig. 5 [22].

F_i^C is a collector control function, which can be defined to identify which node receives water from the collector. F_i^L is a load return control function, which can be denoted to identify which node receives water returning from the adsorption chillers.

$$F_i^C = \begin{cases} 1 & \text{if } i = 1 \text{ and } T_{c,o} \geqslant T_{ta,i} \\ 1, & \text{if } T_{ta,i-1} \geqslant T_{c,o} > T_{ta,i} \\ 0, & \text{otherwise} \end{cases} \tag{4}$$

$$F_i^L = \begin{cases} 1 & \text{if } i = N \text{ and } T_{hw,o} \leqslant T_{ta,N} \\ 1 & \text{if } T_{ta,i} \geqslant T_{hw,o} > T_{ta,i+1} \\ 0, & \text{otherwise} \end{cases} \tag{5}$$

Δm_i is the net flow between nodes, which can either be towards the top or the bottom of the tank, depending on the magnitudes of

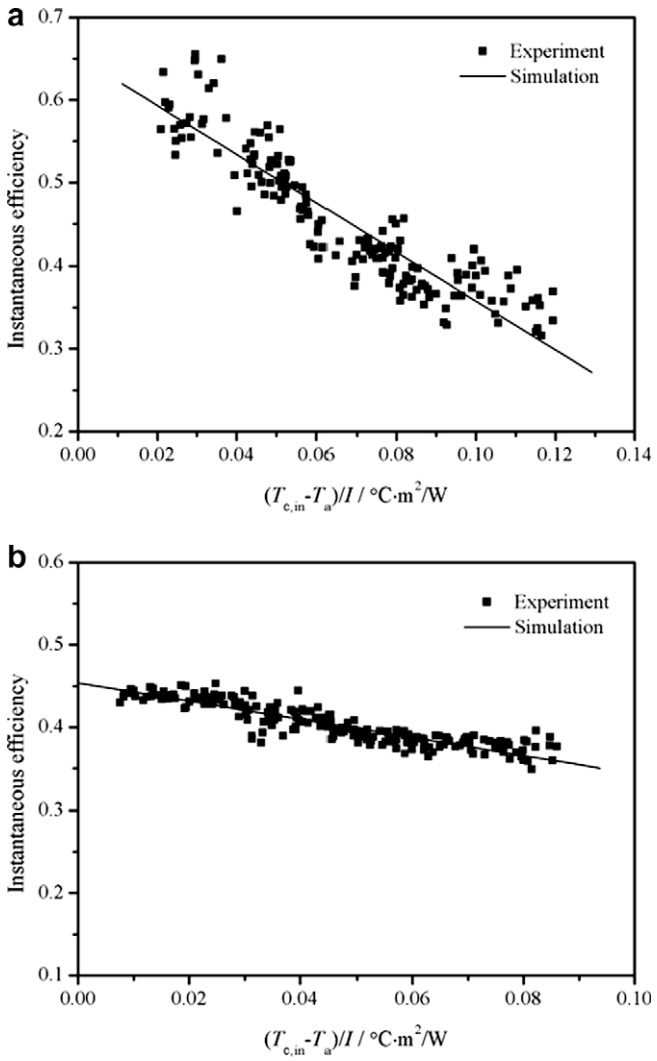

Fig. 4. Experimental data and simulation of instantaneous efficiency for the two solar collector arrays. (a) Heat pipe evacuated tubular solar collector array. (b) U-type evacuated tubular solar collector array.

the collectors flow rate m_c and hot water flow rate to the chillers m_{hw}, and the values of two control functions at any particular instant. It is given as:

$$\Delta m_i = \begin{cases} -m_{hw}\sum_{j=2}^{N} F_j^L, & \text{if } i=1 \\ m_c\sum_{j=1}^{i-1} F_j^C - m_{hw}\sum_{j=i+1}^{N} F_j^L, & \text{if } i=2,\ldots,N-1 \\ m_c\sum_{j=1}^{N-1} F_j^C, & \text{if } i=N \end{cases} \tag{6}$$

Then, the energy balance on each node can be expressed as:

$$\rho_{w,i}A_{ta,se}\Delta x\frac{dT_{ta,i}}{dt} = \left(\frac{U_{ta}A_{ta,si}}{C_{p,w}}\right)_i (T_a - T_{ta,i}) + F_i^C m_c(T_{c,o} - T_{ta,i}) + F_i^L m_{hw}(T_{hw,o} - T_{ta,i}) + \left\{\begin{matrix} \Delta m_i(T_{ta,i-1} - T_{ta,i}) & \text{if } \Delta m_i > 0 \\ \Delta m_{i+1}(T_{ta,i} - T_{ta,i+1}) & \text{if } \Delta m_i < 0 \end{matrix}\right\} \tag{7}$$

3.4. Pipe network of the system without heat storage

In the system without heat storage, taking into account energy gain from the collectors and energy consumed by the adsorption chillers, the energy equation for the pipe network can be expressed as:

$$C_{p,w}\rho_w V_{pn}\frac{dT_{pn}}{dt} = A_{c,hp}I\eta_{c,hp} + A_{c,U}I\eta_{c,U} - C_{p,w}m_{hw}(T_{pn} - T_{hw,o}) \tag{8}$$

3.5. Daily average performance indexes

In the performance analysis, the daily average solar collecting efficiency during the system operation was calculated by:

$$\eta_{ave} = \frac{\int_{D1} A_{c,hp}\eta_{c,hp}Idt + \int_{D1} A_{c,U}\eta_{c,U}Idt}{\int_{D3}(A_{c,hp} + A_{c,U})Idt} \tag{9}$$

The daily average cooling capacity was calculated by:

$$Q_{chill,ave} = \frac{\int_{D2} Q_{chill}dt}{D3} \tag{10}$$

The daily average hot water temperature (hot water supplied to the chillers) was calculated by:

$$T_{hw,ave} = \frac{\int_{D2} T_{hw}dt}{D2} \tag{11}$$

The daily average COP of the system was calculated by:

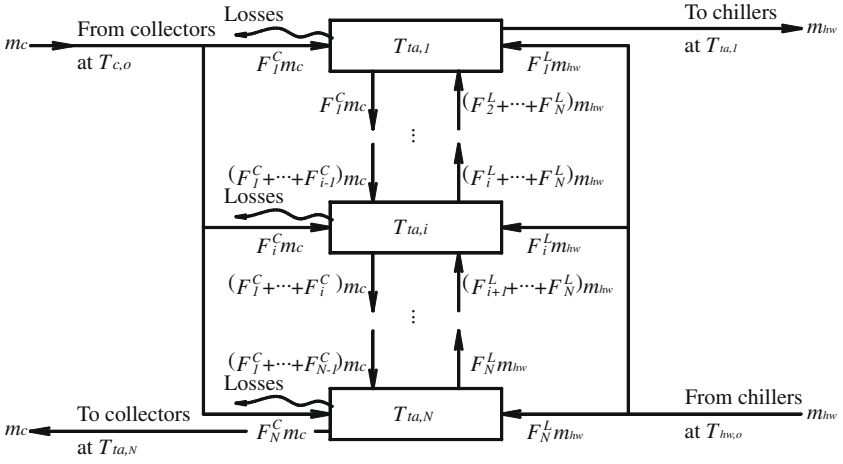

Fig. 5. Simulation model of heat storage water tank.

$$\mathrm{COP}_{ave} = \frac{\int_{D2} Q_{chill} dt}{\int_{D2} Q_{hw} dt} \quad (12)$$

In the above equations, $D1$ is the duration of the solar collecting system operation, $D2$ is the duration of the adsorption chillers operation, and $D3$ represents the working time.

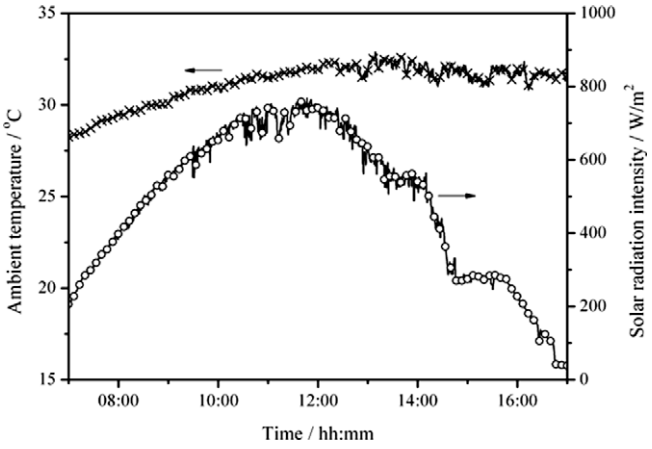

Fig. 6. Variations of solar radiation intensity and ambient temperature.

4. Experimental investigation

4.1. Comparison of operating characteristics between the system with heat storage and the system without heat storage

The experimental results of two days with similar ambient conditions were chosen to compare the operating characteristics of the solar cooling system under different operating modes. The solar cooling system was in operation from 9:00 to 17:00, corresponding to the working schedule of the green building. Fig. 6 shows the variations of ambient temperature and solar radiant intensity during the operating hours. The daily solar insolation was 17.51 MJ/m^2 and the average ambient temperature was 32.56 °C.

Fig. 7 shows the variations of inlet and outlet water temperature for the solar collector arrays under different operating modes, where point 1 represents the automatic start of the solar collecting circulation, point 2 represents the start of the adsorption chillers, and point 3 represents the stop of the adsorption chillers. For the system with heat storage, it was observed that the water temperatures of the inlet and outlet of solar collector array, initially, went up with the increase of solar radiation intensity, approached peak values at noon, and then fell with the decrease of solar radiation intensity. It was also observed that the inlet water temperature curve of the system with heat storage was relatively smooth since

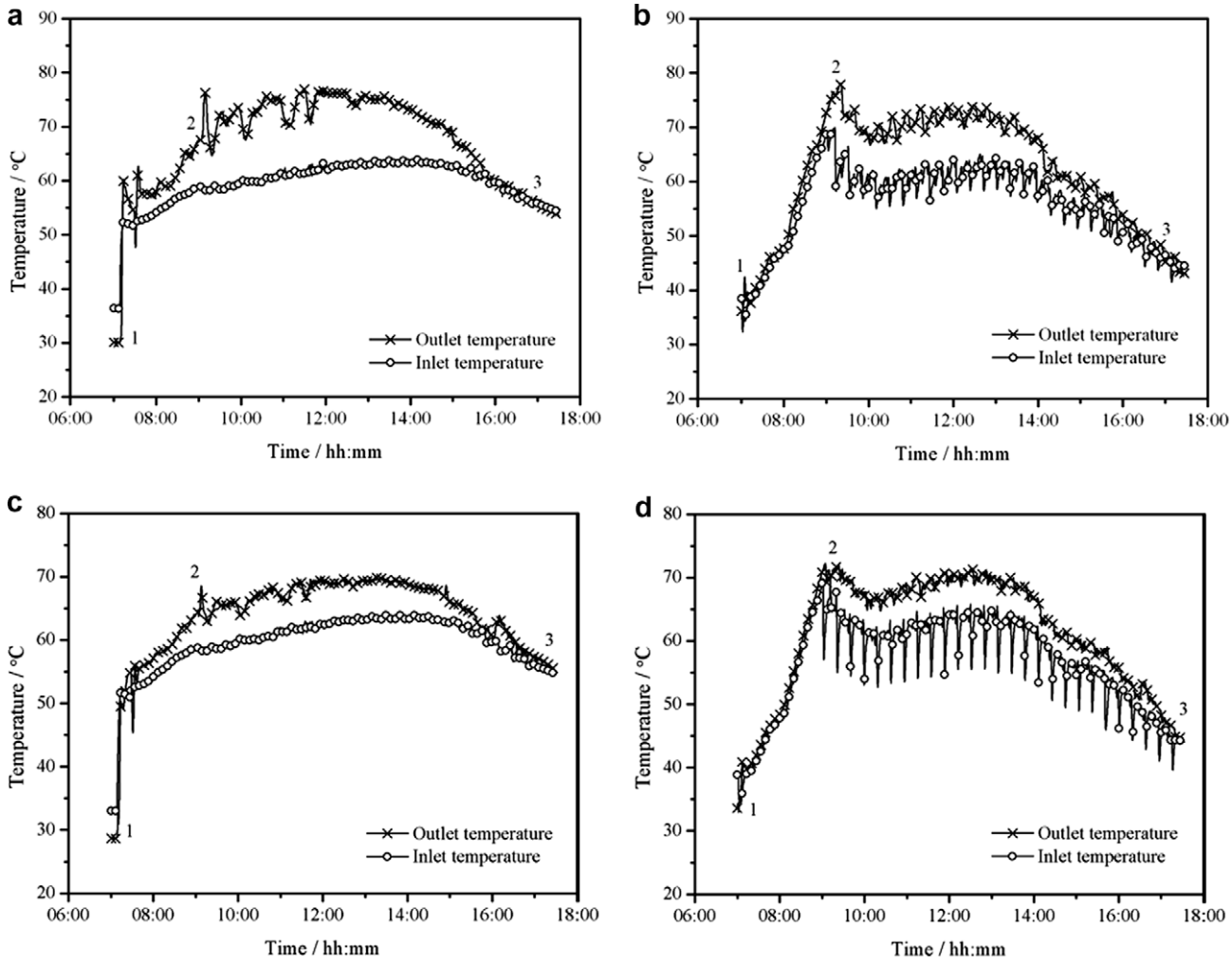

Fig. 7. Variations of inlet and outlet water temperature of the solar collector array. (a) Heat pipe evacuated tubular solar collector array of the system with heat storage. (b) Heat pipe evacuated tubular solar collector array of the system without heat storage. (c) U-type evacuated tubular solar collector array of the system with heat storage. (d) U-type evacuated tubular solar collector array of the system without heat storage.

the water entering the solar collector array came from the bottom of the heat storage water tank.

For the system without heat storage, it was observed that the water temperatures of the inlet and outlet of solar collector array, initially, rose rapidly and reached about 70 °C before 9:00, then fell due to the start-up of two adsorption chillers. From 10:00 to 14:00, the variations of water temperatures of the inlet and outlet of solar collector array were unconspicuous, which indicated the balance between the solar collecting heat and the heat consumption by two adsorption chillers. Afterwards, the water temperatures of the inlet and outlet of solar collector array descended with the decrease of solar radiation intensity. It was interesting to find that the water temperatures of the inlet and outlet of solar collector array cyclically swung since the water entering the solar collector array was directly from the adsorption chillers.

It was concluded that the average water temperature of the inlet of solar collector array in the system without heat storage was 56.52 °C, which was 4 °C lower than that of the system with heat storage. Accordingly, under otherwise identical conditions, the solar collecting efficiency of the system without heat storage was higher than that of the system with heat storage. From the experimental results, it was found that the daily average solar collecting efficiency for the system with heat storage was 37.41%. Comparatively, the daily average solar collecting efficiency for the system without heat storage was 39.95%, which was higher than that of the system with heat storage by 2.54%.

Fig. 8 shows the variations of inlet and outlet water temperature of the adsorption chillers under different operating modes. With regard to the system with heat storage, the inlet water temperature was 62.48 °C when the adsorption chillers were turned on at 9:00, then gradually rose, and approached the peak value of 68.52 °C at 13:30. The rate of temperature rise was 0.02 °C/min during this period of time. From then on, the inlet water temperature fell off with the rate of temperature drop of 0.06 °C/min, and reached 55.49 °C at 17:00 when the adsorption chillers were shut down. By this token, the water temperature at the inlet of the adsorption chillers varied smoothly during 8-h operation of the cooling system. Taking the temperature variations into account, the thermal source driving the adsorption chillers was considered to be stable.

Comparatively, the inlet water temperature of the adsorption chillers varied distinctly in the system without heat storage. From 9:00 to 10:00, because the two adsorption chillers consumed a great deal of heat stored in the pipe network, the inlet water temperature decreased from 72.53 °C to 65.50 °C with a rate of temperature drop of 0.12 °C/min. After 10:00, with the increase of solar radiation intensity, besides meeting the heat consumption by the two adsorption chillers, the solar collector heat was partially stored in the pipe network, which led to the increase of inlet water temperature. At about 12:30, the inlet water temperature of the adsorption chillers reached the peak value of 70.85 °C. From 10:00 to 12:30, the rate of temperature rise was 0.04 °C/min. Whereafter, the inlet water temperature of the adsorption chillers decreased with the decrease of solar radiation intensity. It was concluded that the rate of temperature drop from 12:30 to 14:00 was 0.05 °C/min. During the last 3-h operation, the rate of temperature drop was 0.10 °C/min, which indicated that the heat consumption by the adsorption chillers overwhelmed the solar collector heat. According to temperature variations, it was observed that the thermal source driving the adsorption chillers was relatively stable from 10:00 to 14:00 since the inlet water temperature varied in the order of magnitude of 0.01 °C/min. However, the inlet water temperature varied severely in the order of magnitude of 0.1 °C/min in the other two time-intervals (9:00–10:00 and 14:00–17:00). As a result, the chillers could be considered to be driven by a variable thermal source. In the last hour, although the adsorption chillers were inefficient because the average inlet water temperature was lower than 55 °C, the experiment was carried on in order to compare with the performance of the system with heat storage.

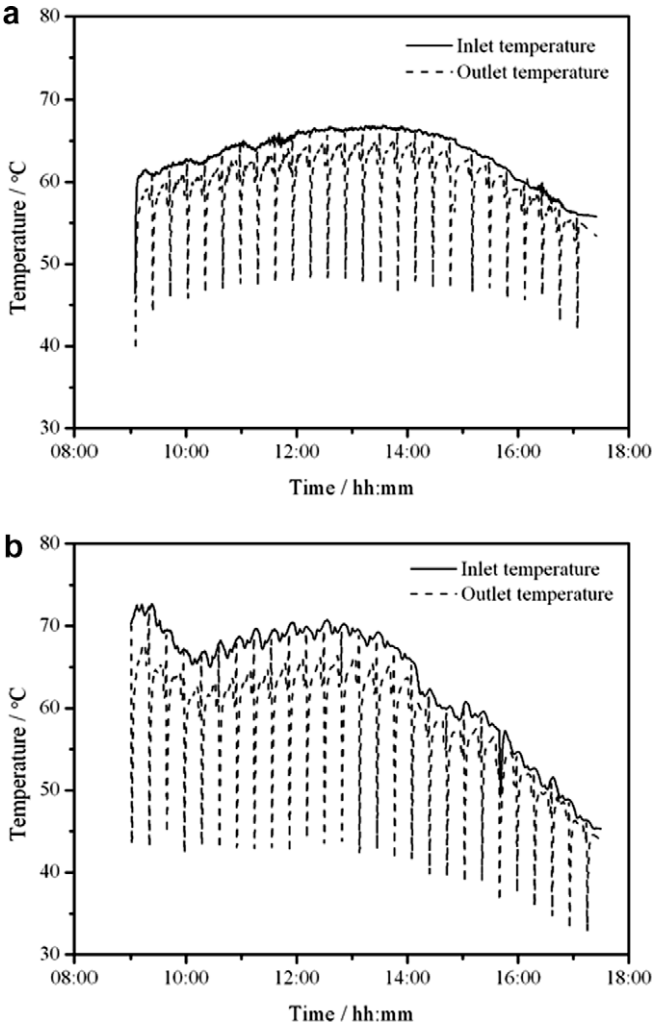

Fig. 8. Variations of inlet and outlet water temperature of the adsorption chillers. (a) The system with heat storage. (b) The system without heat storage.

Although obvious differences of temperature variations could be observed between Fig. 8a and b, the average water temperature of the inlet of the adsorption chillers during 8-h operation was concluded to be about 63.48 °C in the system with heat storage. Comparatively, it was 63.07 °C in the system without heat storage, which approached that of the system with heat storage with a relative error of 0.65%.

Solar energy is a typical variable heat source; furthermore, adsorption refrigeration is characterized by variable behavior. Consequently, the operation of the system without heat storage presents wave character because of low water capacity of the system. However, the system with heat storage is capable of stable operation, owing to the regulating effect of the heat storage water tank.

Fig. 9 shows the variation of temperatures inside the heat storage water tank during the operation of the solar cooling system with heat storage, where point 1 represents the automatic start of the solar collecting circulation, point 2 represents the start of the adsorption chillers, and point 3 represents the stop of the adsorption chillers. From point 1 to point 2, only solar collector circulation was in operation, which led to the increase of water tem-

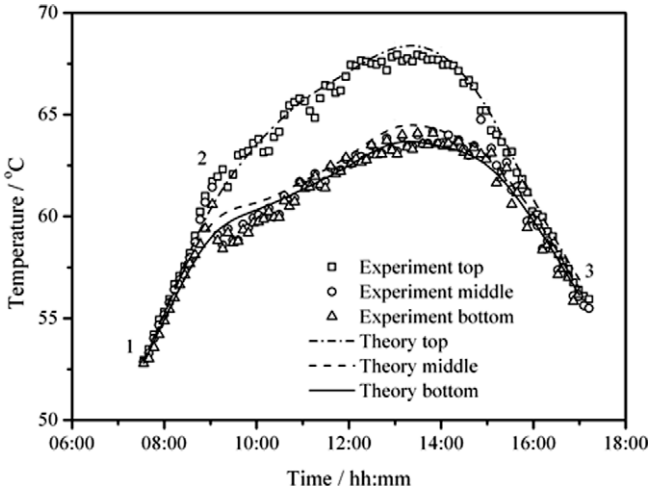

Fig. 9. Variation of water temperatures in the heat storage water tank.

perature without thermal stratification. However, when the adsorption chillers were turned on, thermal stratification could be found. Since the hot water at the top was supplied to the adsorption chillers, thermal stratification helped to improve the performance of the system. The mixing effect of the heat storage water tank assures that the water with relatively uniform temperatures flows into the solar collector array and the adsorption chillers, respectively.

4.2. Performance comparison between the system with heat storage and the system without heat storage

Fig. 10 compares the cooling capacity at different time-intervals between the system with heat storage and the system without heat storage. It was observed that the time-averaged cooling capacity approached the maximal value during the time-interval from 11:00 to 12:00 in the system without heat storage. However, in the system with heat storage, the maximal value of cooling capacity appeared during the time-interval from 13:00 to 14:00, which was two hours later than that of the system without heat storage. It was also observed that, before 12:00, the average cooling capacity of the system without heat storage was higher than that of the system with heat storage by 14.10%. Nevertheless, from 13:00 to 17:00, the average cooling capacity of the system with heat storage was higher than that of the system without heat storage by 9.13%. On all accounts, the daily average cooling capacity was 11. 41 kW in the system with heat storage. However, it was 10.96 kW in the system without heat storage, which was close to that of the system with heat storage with a relative error of 3.94%.

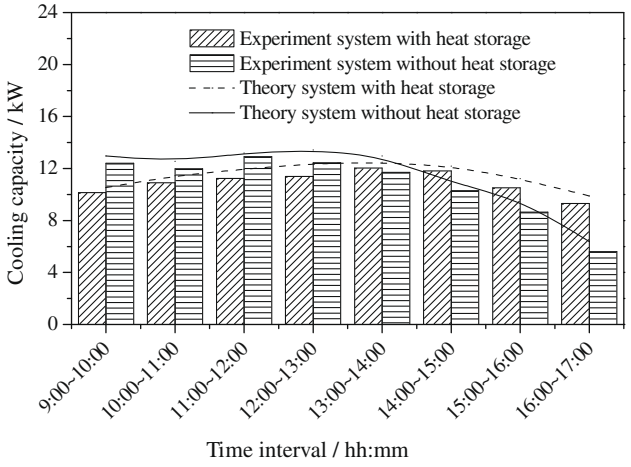

Fig. 10. Comparison of cooling capacity between the system with heat storage and the system without heat storage.

With regard to the heat consumption of the two adsorption chillers, the daily average COP of the system was 0.35 in the system with heat storage. Comparatively, it was 0.34 in the system without heat storage, which was nearly the same as that of the system with heat storage with a relative error of 2.86%.

In the solar cooling system, it is important to reduce electric power consumption; consequently, electrical COP (the ratio of cooling capacity to the power consumption) is another important index to evaluate the performance of the system. In the system with heat storage, considering the solar collecting pump (P1), hot water pump (P2) and cooling water pump (P3), the whole power consumption was 1.87 kW, and the average electrical COP was 6.10 during 8-h operation. Whereas, the whole power consumption in the system without heat storage was 1.32 kW because of no use of the hot water pump (Pump 2). The average electrical COP was 8.30 during 8-h operation, which was 36.07% higher than that of the system with heat storage.

From the above mentioned experiments of the solar adsorption cooling system under different operating modes, it can be seen that the daily average cooling capacity and COP in the system without heat storage was nearly the same as that of the system with heat storage. However, the system without heat storage has the advantage of a higher electrical COP, which is meaningful regarding energy conservation of solar cooling systems.

5. Performance analysis

The main performance indices (daily average solar collecting efficiency, daily average cooling capacity, daily average hot water temperature and daily average COP) of the solar adsorption cooling system were analyzed, making the following assumptions:

(1) The solar radiation intensity and ambient temperature were assumed to keep the same trend as Fig. 6, however, the values varied proportionally by multiplying the values in Fig. 6 by a fixed value.
(2) The inlet temperature of cooling water and chilled water was 32 °C and 15 °C, respectively.
(3) The working time was from 9:00 to 17:00.
(4) In the system with heat storage, the following parameters were used in the analysis: average ambient temperature was 30 °C, volume of the hot water tank was 2.5 m^3 (height-to-diameter ratio of 1.13), distance between nodes Δx in the water tank model was 0.05 m, initial temperature of water in the water tank was 30 °C, mass flow rate of hot water into the chillers was 1.4 kg/s, and mass flow rate of water in the solar collector array was 1.25 kg/s.
(5) In the system without heat storage, the following parameters were used in the analysis: average ambient temperature was 30 °C, volume of hot water in the pipe network was 0.3 m^3, initial temperature of water in the pipe network was 30 °C, and mass flow rate of water in the pipe network was 1.25 kg/s.

5.1. Performance comparison of the solar adsorption cooling system with/without heat storage with daily solar insolation

Solar radiation intensity is the key ambient parameter to influence the performance of the solar cooling system. Fig. 11 compares

the variations of the system performance with daily solar insolation under different operating modes when the solar collector area is 150 m^2. In the system with heat storage, it was observed that the daily average solar collecting efficiency increased with the increase of daily solar insolation, which led to the corresponding improvement of daily average hot water temperature. By comparison, in the system without heat storage, it was observed that the daily average hot water temperature increased with the increase of daily solar insolation, although the daily average solar collecting efficiency decreased with the increase of daily solar insolation. It was also observed that the daily average solar collecting efficiency of the system without heat storage was higher than that of the system with heat storage. This can be attributed to the fact that the inlet water temperature of the solar collector array in the system without heat storage is relatively lower because the inlet water of the solar collector array comes from the outlet of the adsorption chillers.

The adsorption chillers were powered by the thermal source; therefore, the hot water temperature becomes a key factor to improve the performance. As shown in Fig. 9, either in the system with heat storage or in the system without heat storage, the daily average cooling capacity and COP similarly increased with the increase in daily solar radiation. It was also shown that the daily average cooling capacity of the system without heat storage went beyond that of the system with heat storage when the daily solar radiation exceeded 18 MJ/m^2. Accordingly, the daily average COP of the system without heat storage was a little higher than that of the system with heat storage when the daily solar radiation exceeded 18 MJ/m^2. Consequently, it can be seen that the system without heat storage has more potential in areas with abundant solar energy resources.

5.2. Performance comparison of the solar adsorption cooling system with/without heat storage with solar collector area

Fig. 12 compares the variations of the system performance with solar collector area under different operating modes when daily solar insolation is 18 MJ/m^2. In the system with heat storage, it was seen that the daily average hot water temperature increased with the increase in solar collector area, because more heat was collected in the heat storage water tank, correspondingly, the daily average cooling capacity and COP went up. However, the daily average solar collecting efficiency decreased with the increase in solar collector area. Similar variations of the system performance with solar collector area could be seen in the system without heat storage. Consequently, in practical solar adsorption cooling systems, solar collector area should be determined according to the design condition. It is suggested that too many solar collectors not only lead to the reduction of solar collecting efficiency but also increase the initial cost of the system. It was also found that the

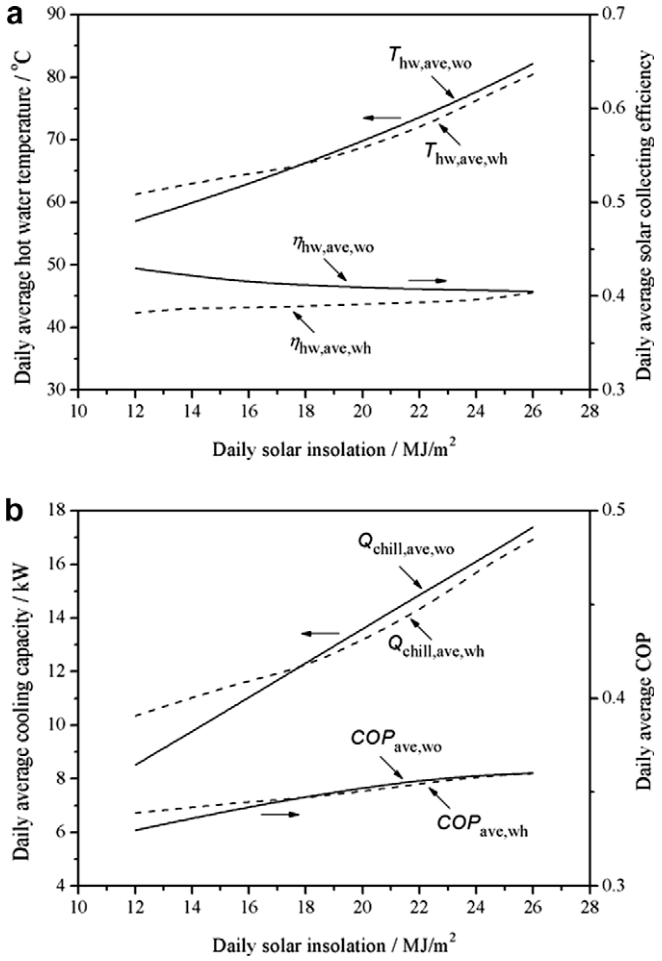

Fig. 11. Comparison of system performance with daily solar insolation between the system with heat storage and the system without heat storage. (a) Daily average hot water temperature and daily average solar collecting efficiency versus daily solar insolation. (b) Daily average cooling and daily average COP versus daily solar insolation.

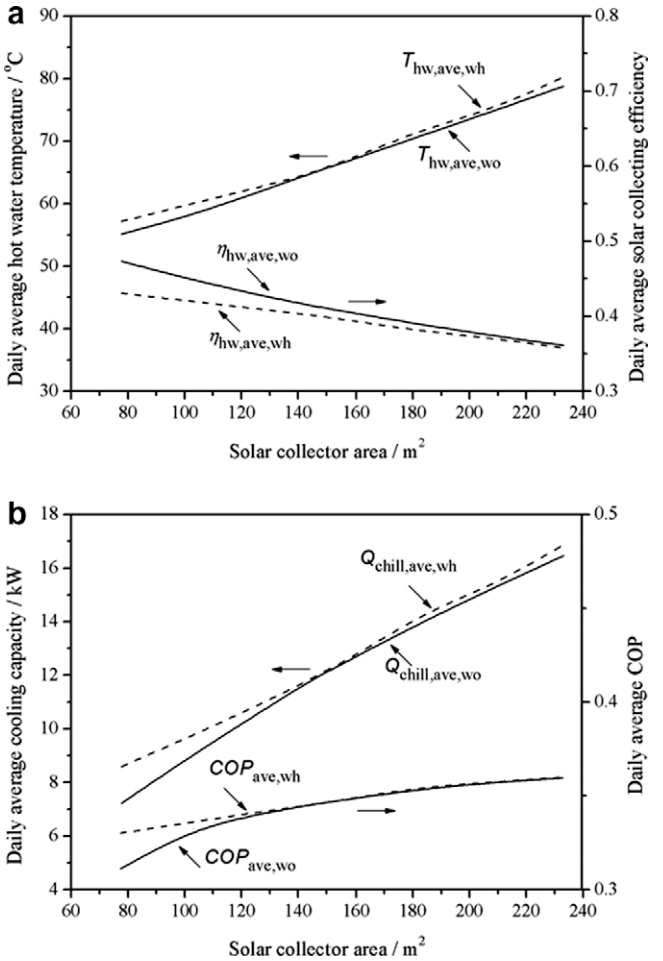

Fig. 12. Comparison of system performance with solar collector area between the system with heat storage and the system without heat storage. (a) Daily average hot water temperature and daily average solar collecting efficiency versus solar collector area. (b) Daily average cooling and daily average COP versus solar collector area.

system performance of the system without heat storage approached that of the system with heat storage when the solar collector area exceeded 150 m^2. As a result, if it is impossible to install a heat storage water tank in the design of a solar adsorption cooling system, it is suggested to choose a system without heat storage by means of the increment of solar collector area for the purpose of achieving the similar cooling effect as that of the system with heat storage.

5.3. Performance analysis of the effect of heat storage water tank on the solar adsorption cooling system with heat storage

Fig. 13 shows variations of the system performance with volume of water tank (height-to-diameter ratio of 1.13) when the daily solar insolation was 18 MJ/m^2. Under identical conditions, water temperature in the heat storage water tank decreased with the increase of volume, therefore, the daily average solar collecting efficiency increased. However, both daily average cooling capacity and COP varied inversely. In our solar adsorption cooling project of the green building of Shanghai Institute of Building Science, the ratio of water tank volume to solar collector area was about 0.02 m^3/m^2, which was testified to be suitable for the system operation.

Fig. 14 indicates variations the system performance with height-to-diameter ratio of water tank when the daily solar insolation was 18 MJ/m^2. In this case, the volume of hot water tank was kept at 2.5 m^3. It was seen that both the daily average solar collecting efficiency and hot water temperature could be enhanced by the increase in height-to-diameter ratio of water tank. This can be attributed to the fact that increase of height-to-diameter ratio of the water tank leads to a better thermal stratification in the water tank. As a result, both the daily average cooling capacity and COP increased with the increase in height-to-diameter ratio of water tank. In practical solar cooling projects, the partitioned water tanks are more favorable than such whole-tanks [11].

Nondimensional mass flow rate was calculated as the ratio of mass flow rate of water in the solar collector arrays to the mass flow rate of hot water into the chillers. Fig. 15 shows variations the system performance with the nondimensional mass flow rate. In this case, the mass flow rate of hot water into chillers was 1 kg/s. It can be observed clearly that the optimum value of the nondimensional mass flow rate was 1.3, which corresponded to the maximal daily average hot water temperature and the corresponding daily average cooling capacity. Such a phenomenon can be due to two reasons; for one thing, a better energy matching between the solar collectors and the adsorption chillers is achieved, for another, such a nondimensional mass flow rate leads to a better thermal stratification in the water tank. Additionally, simulation was carried out with different mass flow rate of hot water into chillers, and similar trends were obtained.

The variation of the optimum nondimensional mass flow rate with the specific mass flow rate is illustrated in Fig. 16. The specific mass flow rate was defined as the mass flow rate of hot water into chillers per unit of solar collector area. It was observed that opti-

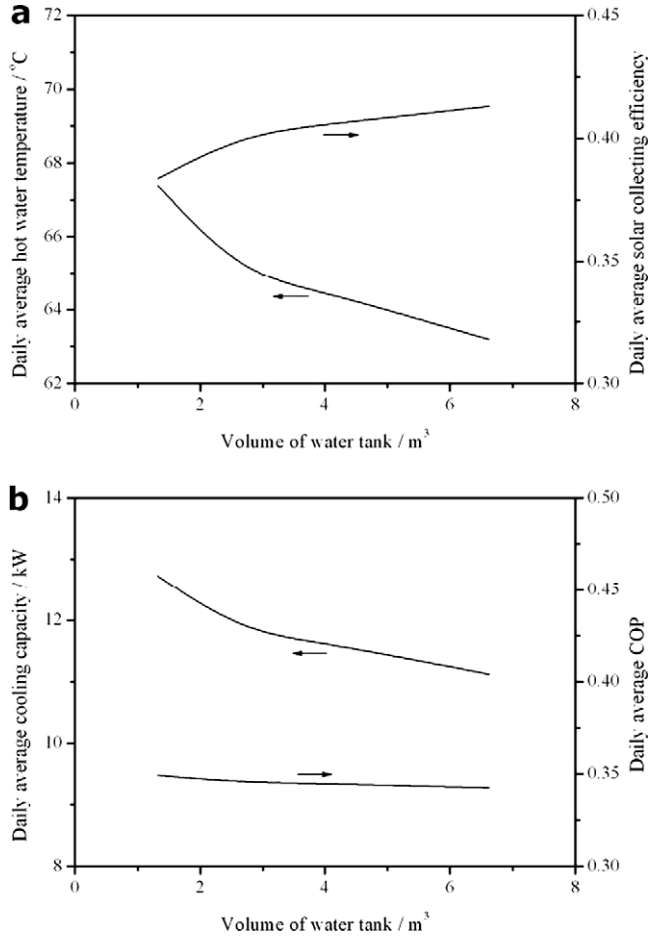

Fig. 13. System performance with volume of water tank. (a) Daily average hot water temperature and daily average solar collecting efficiency versus volume of water tank. (b) Daily average cooling capacity and daily average COP versus volume of water tank.

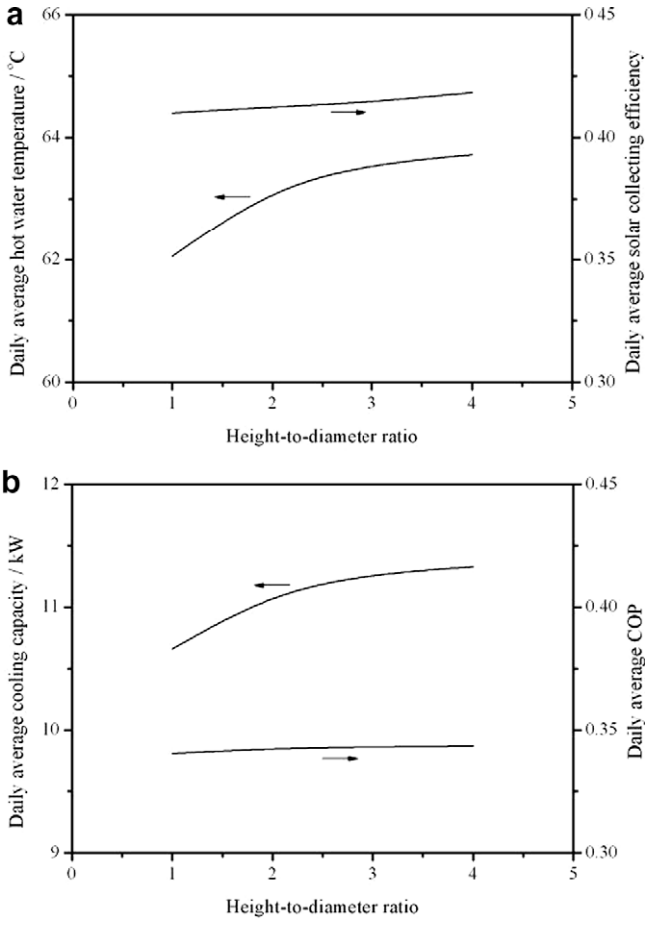

Fig. 14. System performance with height-to-diameter ratio of water tank. (a) Daily average hot water temperature and daily average solar collecting efficiency versus height-to-diameter ratio of water tank. (b) Daily average cooling capacity and daily average COP versus height-to-diameter ratio of water tank.

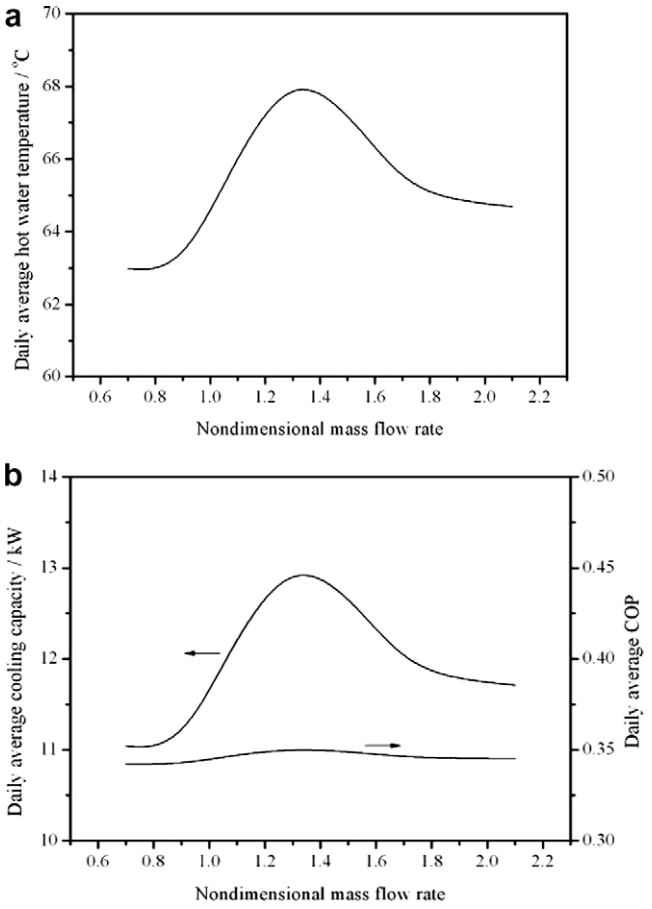

Fig. 15. System performance with nondimensional mass flow rate. (a) Daily average hot water temperature versus nondimensional mass flow rate. (b) Daily average cooling capacity and daily average COP versus nondimensional mass flow rate.

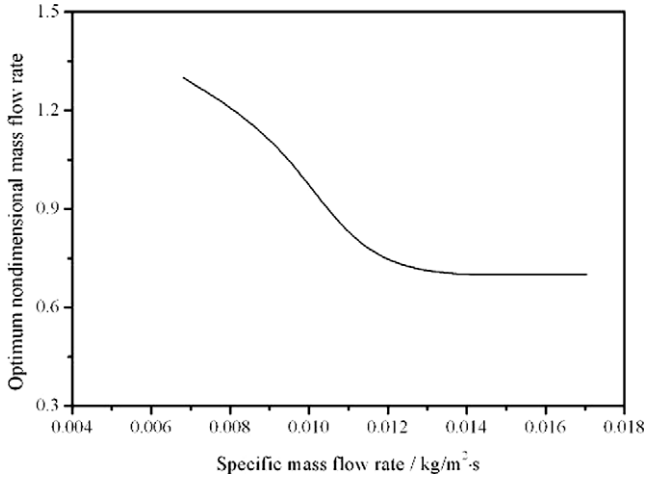

Fig. 16. Variation of optimum nondimensional mass flow rate with specific mass flow rate.

mum nondimensional mass flow rate decreased with the increase of specific mass flow rate. The optimum value approaches 0.7 when the specific mass flow rate exceeds 0.012 kg/m^2 s. This conclusion is especially helpful for the design and optimization of solar adsorption cooling system.

6. Conclusions

A solar adsorption cooling system which can be switched between a system with heat storage and a system without heat storage was designed. Experiments were carried out to compare the operating characteristics of the system under these two operating modes. As a brief summary, it is wished to emphasize the most significant aspects of this work in the following.

(1) The comparison of the operating characteristics between the system with heat storage and the system without heat storage shows that the system with heat storage operates stably because of regulating effect by the heat storage water tank. However, under otherwise similar conditions, the system without heat storage is capable of obtaining similar cooling effect as that of the system with heat storage although it has an obvious varying character.
(2) Compared with the system with heat storage, the system without heat storage has the advantage of higher solar collecting efficiency. Moreover, the energy-saving effect of the system without heat storage is more notable due to a higher electrical COP.
(3) By comparison, the system without heat storage is more suitable for areas with abundant solar energy resources.
(4) Comparatively, the pipe network of the system without heat storage has the advantage of simplicity because of no use of the heat storage water tank. Through increasing the solar collector area, the system without heat storage is capable of achieving a similar cooling effect to the system with heat storage.

Acknowledgements

This work was supported by National Natural Science Foundation of China under the contract No. 50876064 and Special Fund of Higher Education Doctorate Subject under the contract No. 200802481115.

References

[1] Henning Hans-Martin. Solar assisted air conditioning of buildings – an overview. Appl Therm Eng 2008;27(10):1734–49.
[2] Casals Xavier García. Solar absorption cooling in Spain: perspectives and outcomes from the simulation of recent installations. Renew Energy 2006;31(9):1371–89.
[3] Kumar Pradeep, Devotta S. Modelling of the thermal behaviour of a solar regenerator for open-cycle cooling systems. Appl Energy 1989;33(4):287–95.
[4] Muneer T, Uppal AH. Modelling and simulation of a solar absorption cooling system. Appl Energy 1985;19(3):209–29.
[5] Mateus Tiago, Oliveira Armando C. Energy and economic analysis of an integrated solar absorption cooling and heating system in different building types and climates. Appl Energy 2009;86(6):949–57.
[6] Desideri Umberto, Proietti Stefania, Sdringola Paolo. Solar-powered cooling systems: technical and economic analysis on industrial refrigeration and air-conditioning applications. Appl Energy 2009;86(9):1376–86.
[7] Ali Ahmed Hamza H, Noeres Peter, Pollerberg Clemens. Performance assessment of an integrated free cooling and solar powered single-effect lithium bromide–water absorption chiller. Sol Energy 2008;82(11):1021–30.
[8] Pongtornkulpanich A, Thepa S, Amornkitbamrung M, Butcher C. Experience with fully operational solar-driven 10-ton LiBr/H_2O single-effect absorption cooling system in Thailand. Renew Energy 2008;33(5):943–9.
[9] Rodríguez Hidalgo MC, Rodríguez Aumente P, Izquierdo Millán M, Lecuona Neumann A, Salgado Mangual R. Energy and carbon emission savings in Spanish housing air-conditioning using solar driven absorption system. Appl Therm Eng 2008;28(14–15):1734–44.
[10] Syed A, Izquierdo M, Rodríguez P, Maidment G, Missenden J, Lecuona A, et al. A novel experimental investigation of a solar cooling system in Madrid. Int J Refrig 2005;28(6):859–71.
[11] Li ZF, Sumathy K. Experimental studies on a solar powered air conditioning system with partitioned hot water storage tank. Sol Energy 2001;71(5):285–97.

[12] Balaras Constantinos A, Grossman Gershon, Henning Hans-Martin, Infante Ferreira Carlos A, Podesser Erich, Wang Lei, et al. Solar air conditioning in Europe-an overview. Renew Sust Energy Rev 2007;11(2):299–314.
[13] Wang RZ, Oliveira RG. Adsorption refrigeration-An efficient way to make good use of waste heat and solar energy. Prog Energy Combust 2006;32(4): 424–58.
[14] Alghoul MA, Sulaiman MY, Sopian K, Azmi BZ. Performance of a dual-purpose solar continuous adsorption system. Renew Energy 2009;34(3):920–7.
[15] Khattab NM. Simulation and optimization of a novel solar-powered adsorption refrigeration module. Sol Energy 2006;80(7):823–33.
[16] Saha BB, Koyama S, Kashiwagi T, Akisawa A, Ng KC, Chua HT. Waste heat driven dual-mode, multi-stage, multi-bed regenerative adsorption system. Int J Refrig 2003;26(7):749–57.
[17] Yong Li, Sumathy K. Modeling and simulation of a solar powered two bed adsorption air conditioning system. Energy Convers Manage 2004;45(17): 2761–75.
[18] Saha BB, Akisawa A, Kashiwagi T. Solar/waste heat driven two-stage adsorption chiller: the prototype. Renew Energy 2001;23(1):93–101.
[19] Liu YL, Wang RZ, Xia ZZ. Experimental study on a continuous adsorption water chiller with novel design. Int J Refrig 2005;28(2):218–30.
[20] Zhai XQ, Wang RZ, Dai YJ, Wu Y, Xu YX, Ma Q. Solar integrated energy system for a green building. Energy Build 2007;39(8):985–93.
[21] Wang DC, Wu JY, Xia ZZ. Study of a novel silica gel–water adsorption chiller. Part II. Experimental study. Int J Refrig 2005;28(7):1084–91.
[22] Li ZF, Sumathy K. Simulation of a solar absorption air conditioning system. Energy Convers Manage 2001;42(3):313–27.